INSTITUTE OF PHYSICS PUBLISHING PLASMA SOURCES SCIENCE AND TECHNOLOGY
Plasma Sources Sci. Technol. **14** (2005) 692–699 doi:10.1088/0963-0252/14/4/008

Investigation of the density and temperature of electrons in a compact 2.45 GHz electron cyclotron resonance ion source plasma by x-ray measurements

Markus Hohl, Peter Wurz and Peter Bochsler

Physikalisches Institut, University of Bern, CH-3012 Bern, Switzerland

Received 25 March 2004
Published 4 October 2005
Online at stacks.iop.org/PSST/14/692

Abstract
X-ray measurements of the plasma of a compact 2.45 GHz electron cyclotron resonance ion source (ECRIS) are performed to determine the temperature and density of the electrons heated resonantly in the ECRIS. The x-ray detector used to investigate the plasma consists of a small silicon (Si-PIN) photodiode to detect photons in the energy range of 1–100 keV. The detector has an energy resolution of 180 eV at 5.9 keV that allows us to record detailed x-ray spectra. Assuming two temperature electron populations, both Maxwellian distributed, the analysis of the x-ray spectra shows a temperature of about 2 keV for the hot electron fraction in addition to the population of cold electrons at less than 2 eV. The fraction of the hot electrons amounts to 1–10%. We present a description of the x-ray detector set-up as well as x-ray spectra and calculations for the temperature and density of the electrons in the ECRIS plasma.

1. Introduction

Electron cyclotron resonance ion sources (ECRISs) are well known for efficiently producing highly charged ions. In a continuous plasma discharge electrons are heated up by microwave radiation and are then used to ionize neutrals and ions step by step. Basically, in an ECRIS plasma two or more electron populations with different kinetic energies coexist, depending on their location in the magnetic confinement (e.g. see the book by Geller [1]). Electrons near or in the ECR-resonance zones can have energies that are up to several orders of magnitude higher than the bulk electrons located far away from the resonance zones, e.g. in the middle of the plasma volume or near its edges. For simplicity, the electron populations are often divided into a hot and a cold population depending on the kinetic energies of the electrons. The ability to produce highly charged ions strongly depends on the temperature and the density of the two populations. Both parameters affect the ionization and recombination rates of ions and are therefore crucial parameters for the performance of the ion source [2]. We measured these two parameters in order to improve our understanding and possibly increase the performance of our ECR source.

The plasma that we investigated is a continuous plasma in an ECRIS operating at 2.45 GHz with a permanent magnetic confinement [3, 4]. The highly compact assembly of the magnetic structure, which completely surrounds the plasma tube at a diameter of 6.6 cm, allows no access for direct observation of the hot plasma. Furthermore the arrangement does not allow the installation of any magnetic or electric probes and coils inside the plasma tube because the plasma is too hot, and there is not enough space left to locate them between the plasma discharge and the tube wall. The experimental set-up and the x-ray detector implementation will be discussed in the next section in detail.

Plasma diagnostic tools that need to receive electromagnetic waves sent through the plasma, such as plasma particle flux measurements or scattering of electromagnetic waves, cannot be performed as well, even if there are no probes to be placed into the plasma chamber. The problem is again the lack of space to accommodate a transmitter to send electromagnetic waves and a receiver to receive them.

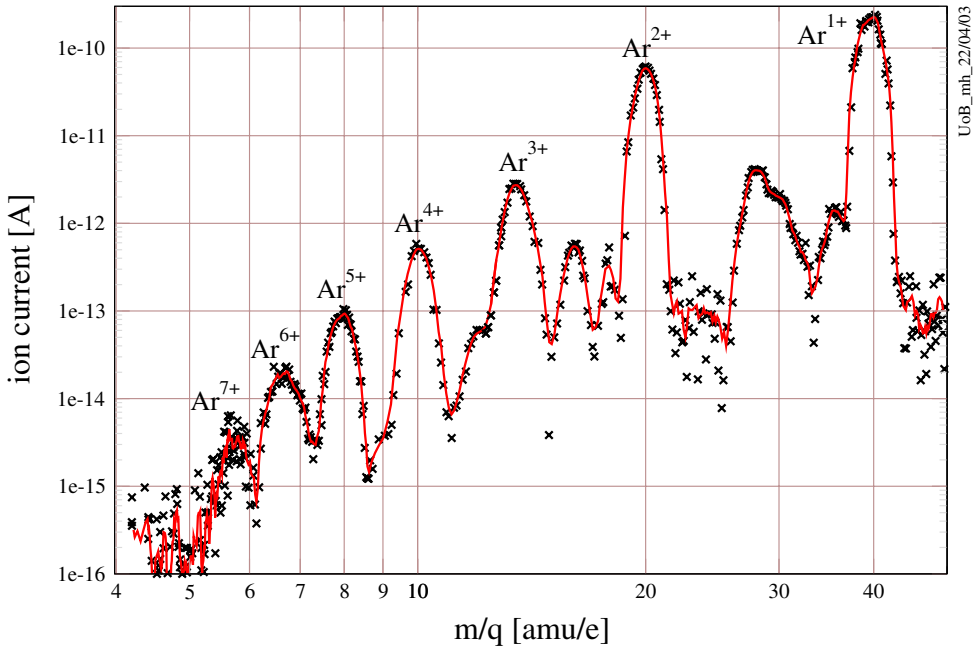

Figure 1. Typical argon spectrum showing all the charge states in the extracted ion beam measured with a Faraday cup. The straight line represents a five point average of the measured data. Other mass peaks arise from residual gas in the ion source.

Thus, there remain only the spectroscopic diagnostic tools, such as the detection of electromagnetic waves emitted by free and bounded electrons from the plasma discharge. The advantage of these diagnostic techniques is that there is no need to measure the radiation in the immediate vicinity of the hot plasma. The measurements can be performed remotely, at a certain distance from the plasma, without loss of accuracy, although the radiation intensity decreases with distance. Nevertheless, it is important to have a direct view of the plasma to be sure to measure the radiation coming from the plasma and not from an effect initiated by photons, e.g. photons hitting the plasma chamber, which can cause emission of photons with a certain energy (x-ray fluorescence).

To the best of our knowledge nobody has ever measured the electron temperature and density in such a small and compact 2.45 GHz ECRIS. Of course there exist values from several ECRIS models and measurements from comparable sources, but these sources are not that compact or work at higher frequencies [5–9].

In figure 1 a measurement of the extracted ion beam using a Faraday cup is given showing all the charge states of argon extracted from an argon plasma. Ion currents in the pA-range are well matched to our application of calibrating space plasma instrumentation. The rather small ion currents for higher charged argon ions are problematic since the fraction of contamination of residual gas ions is often several times higher than the desired ion species, which makes the calibration of instrumentation almost impossible [4, 10]. Before installing the x-ray detector such measurements were the most essential, and basically, the only information we had about our ECR plasma. We estimated the temperature of the electrons in the plasma [11] with a simple plasma model for which we solved ion balance equations by taking only ionization and recombination into account. The ratios of the peak height yielded estimates for the electron temperature in the plasma. The present x-ray measurements showed that our model results underestimated the electron temperature, and according to the new data we set-up a second and more sophisticated plasma model [10].

From the fact that we could extract beams of Ar^{7+} ions, which has an ionization potential of more than 140 eV, a very hot electron population seems to prevail. Our x-ray measurements reveal a typical temperature of about 2 keV assuming a Maxwellian distribution for the kinetic energies of the electrons. For the hot population we found a density in the range of 1×10^{10} cm^{-3}. Having a typical value of 2 keV for the Maxwellian distribution, very hot electrons with energies up to several tens of kiloelectronvolts can be expected.

In the next section we start with a detailed description of the experimental set-up and the performance of the x-ray detector. Then a recorded x-ray spectrum is given followed by a derivation of the electron temperature and density. Finally, this work is completed with a comparison of already published temperatures and densities with our measured ones.

2. Experimental set-up

The design of the compact ECRIS is based on an earlier development of the University of Giessen, Germany [3]. It mainly consists of a plasma tube surrounded by three magnet rings consisting of six magnets each, a gas and microwave inlet and an ion extraction electrode. An additional vacuum tube that accommodates the x-ray detector inside the vacuum environment is closely attached to the plasma chamber (see figure 2). A detailed description of the MEFISTO ECRIS is given by Marti *et al* [4]. The ECRIS is part of a solar plasma calibration facility used to develop, test and calibrate space plasma instrumentations, especially for instruments which are designed to detect solar plasma particles [10].

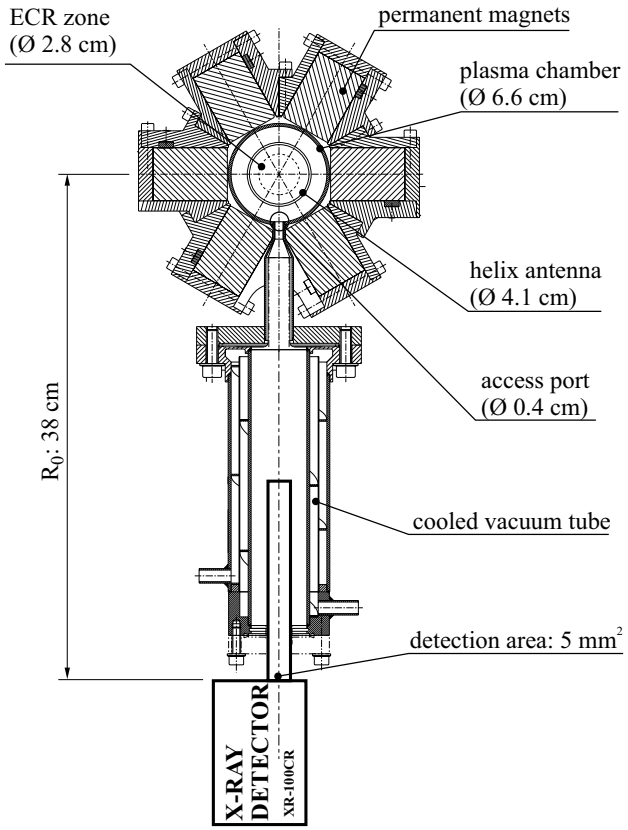

Figure 2. The x-ray detector, a Si (PIN) type solid state detector with a cooled active detection area of 5 mm^2, is mounted in a tube closely attached to the plasma chamber allowing for a direct view of the hot plasma.

The plasma discharge occurs in a tube with a diameter of 6.6 cm and a length of 36.5 cm. A PID-regulated Piezo-valve allows for the controlled inlet of gaseous elements as operating gas for the plasma discharge. The valve together with a reference volume and an orifice leading into the plasma chamber precisely controls the gas inflow to maintain a constant gas pressure for stable operation. The microwave radiation is coupled from the waveguide via a coaxial adaptor into the plasma chamber with a helix antenna. The antenna emits right-hand circular polarized (RHCP) electromagnetic waves to resonantly heat the electrons. Heating occurs in the resonance zones of the magnetic bottle, which is created with 18 permanent magnets arranged in three rings. Each ring consists of six Fe–Nd–B magnetic blocks fixed in a hexagonal structure. The magnetic bottle confines electrons and ions and provides a resonance zone for the electron heating. The ions are extracted through the loss cone of the bottle by a puller electrode and are accelerated with a potential of 3 kV, resulting in a kinetic energy of 3 keV per charge.

The x-ray detector is mounted on a CF-40 flange, which is attached to the cooled vacuum tube using a standard Conflat compression O-ring port. In this way, the electronics of the detector can be located outside the vacuum with an extended small tube housing the actual detector at its end passing through the O-ring port into the vacuum. The O-ring port allows the operation of the detector in a vacuum of a pressure of 10^{-8} mbar. The access port points directly to the core of the hot plasma (see figure 2) allowing the detector a direct view of the plasma to detect x-rays originating from the plasma discharge. Photons are also emitted through x-ray fluorescence that takes place when photons are absorbed by the chamber walls. These x-ray fluorescence effects have characteristic energies producing spectra with a line structure (see figure 3).

The x-ray detector is a commercial state-of-the-art detector (XR-100CR, Amptek, USA) that consists of a silicon (Si-PIN) photodiode to detect the x-ray radiation. The detector has an active area of 5 mm^2 with a silicon crystal having a thickness of 500 μm. The x-ray radiation enters the detector through a vacuum tight beryllium (Be) window of 12.5 μm thickness. For good energy resolution of the detector and for a low electronic noise, the Si crystal and the input preamplifier, a FET transistor, attached next to the Si photodiode, are cooled to a temperature of about -30 °C. The arrangement has an energy resolution of $\Delta E = 180$ eV (FWHM) at 5.9 keV at best and a typical background count rate of less than 3×10^{-3} s^{-1} from 2 keV up to 150 keV. The manufacturer recommended usable energy range spans from 2 to 90 keV with a lower limit of 1 keV and an upper limit of 100 keV.

X-rays entering the detector interact with the silicon atoms and create electron/hole pairs for every 3.62 eV of energy lost in the silicon-crystal. A 100 V bias voltage is applied across the silicon to facilitate the electron/hole collection process. Mainly two processes deposit energy in the Si detector, depending on the energy of the photons: for low energies ($h\nu < 40$ keV) the photoelectric effect dominates, and for higher energies ($h\nu > 40$ keV) the photons also undergo Compton scattering.

The detection of the photons depends on their energy and on the dominant energy loss processes; thus the detector does not produce uniform detection efficiency over the whole energy range. The low energy portion is dominated by the thickness of the beryllium window, while the high energy portion is dominated by the active depth of the Si detector. We used the detection efficiency data provided by the manufacturer for the full energy range to convert the measured count rates into photon fluxes.

We performed an energy calibration by comparing measured americium (^{241}Am) spectra with spectra reported in the literature [12]. ^{241}Am is a radioactive isotope with a half-life of 433 years with a dominant γ-decay producing photons with an energy of 59.5 keV. All α-decays with energies in the MeV range cannot be detected since the energy range of the detector is restricted to 100 keV by its thickness. There are two more γ-peaks at the energies 13.95 and 17.74 keV, the Np $L_{\alpha 1}$ and Np $L_{\beta 1}$ transitions, respectively. With these three peaks the whole energy range of the detector was calibrated and was found to be better than 5% in our measurements.

3. Measurements

A typical x-ray spectrum of an argon plasma recorded with the x-ray detector is given in figure 3. Panel (*a*) shows an exponential decay of the intensity with energy and sharp lines at 2.9, 6.4, 7.06 and 10 keV. The prominent peak at 2.9 keV is due to line radiation, representing the argon (Ar) $K_{\alpha 1}$ transition. If we zoom into the spectrum (figure 3, panel (*b*)) the Ar $K_{\beta 1}$ transition can be identified. The two peaks at 6.4 and 7.06 keV

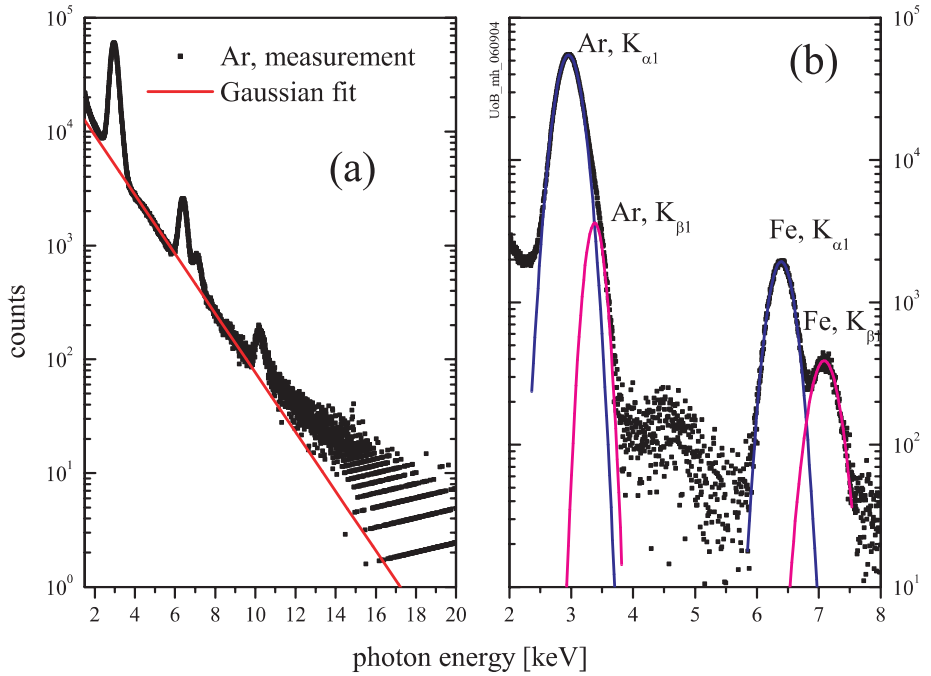

Figure 3. X-ray spectrum generated by an argon plasma in a 2.45 GHz ECR ion source. Panel (*a*): full spectrum with some typical lines produced by different radiation processes: line radiation for the Ar $K_{\alpha1}$ and $K_{\beta1}$ peaks, x-ray fluorescence for the Fe $K_{\alpha1}$ and $K_{\beta1}$ peaks and possibly radioactive radiation emitted by a not yet identified source for the peak at 10 keV. Panel (*b*): expanded view of the Ar and Fe lines.

are emitted line radiation from the transitions $K_{\alpha1}$ and $K_{\beta1}$ in iron (figure 3, panel (*b*)). Iron is not a component of the plasma discharge but the main component of the antenna and the walls of the plasma tube. The small peak at 10 keV is not produced by a process taking place in the plasma, since the peak exists even when no plasma discharge is running. We could not localize the source of this line. It may be generated by a radioactive element contained in the rare earth material of the permanent magnets, or it could be an electronically triggered background effect.

3.1. Electron temperature

The electron temperature, T_e, can be determined from the bremsstrahlung spectrum, i.e. the exponential decay of the intensity with increasing photon energy is interpreted as volume bremsstrahlung from the plasma. In our measurements the spectra show deviations from a strictly exponential decay (aside from the line radiation) at the lower and at the higher end of the energy range. At the low energy side the measurement suffers from background noise that dominates the sprectrum below 2 keV. This noise is also seen in spectra when the plasma was not operated. At the high energy side, the deviation from a simple exponential decay of one hot electron population is interpreted as a second, much hotter, population of the electron distribution, T_{e2}. Unfortunately, this second population has energies which are mostly outside our measurement range and thus cannot be investigated further. For these reasons, we have to constrain our analysis of the bremsstrahlung spectrum to energies above 3 keV and below 10 keV.

Multiple electron populations have been observed in x-ray spectra from ECR plasmas before, e.g. [5–7], and sophisticated analysis algorithms have been designed for the interpretation of these bremsstrahlung spectra extending to energies up to 1 MeV [6, 13]. Since we have a very restricted energy range compared with these earlier investigations, and since the spectrum is dominated by one population in this energy range we made a much simpler analysis to derive an estimate for the temperature of the electron population.

Assuming a Maxwellian distribution for the kinetic energy of the electrons the intensity of the bremsstrahlung is [5,8,16]

$$I(\omega) = A_0 \exp(-\hbar\omega/k_B T_e). \quad (1)$$

If the measured intensities, represented by count rates, are displayed on a logarithmic scale, the slope of the line fitted to the spectrum indicates the temperature of the hot electrons (see the line in figure 3 panel (*a*)). Of course, this method gives only an estimate for the mean energy of the hot electrons. If the interest were in the exact electron distribution functions more sophisticated analysis methods would have to be used [5,6,13], which is beyond the scope of this work.

The data show that the slope of the x-ray spectrum is not exactly exponential, because of the noise contribution at low energies and because the energy distribution of the electrons is not a single Maxwellian, but arises from two hot electron populations, which has been discussed above. Furthermore, there are processes such as line radiation or radioactive radiation, which contribute to the intensity by creating extra counts. These extra counts and the energy distribution of the second population affect the shape of the energy spectra. To get an accurate value for the temperature of the electrons, all the large peaks appearing in the spectrum have to be excluded from the fit. Thus, for the spectrum in figure 3 we had to subtract the peaks from the line radiation at 2.9, 6.4 and 7.06 keV, and an exponential curve was fitted

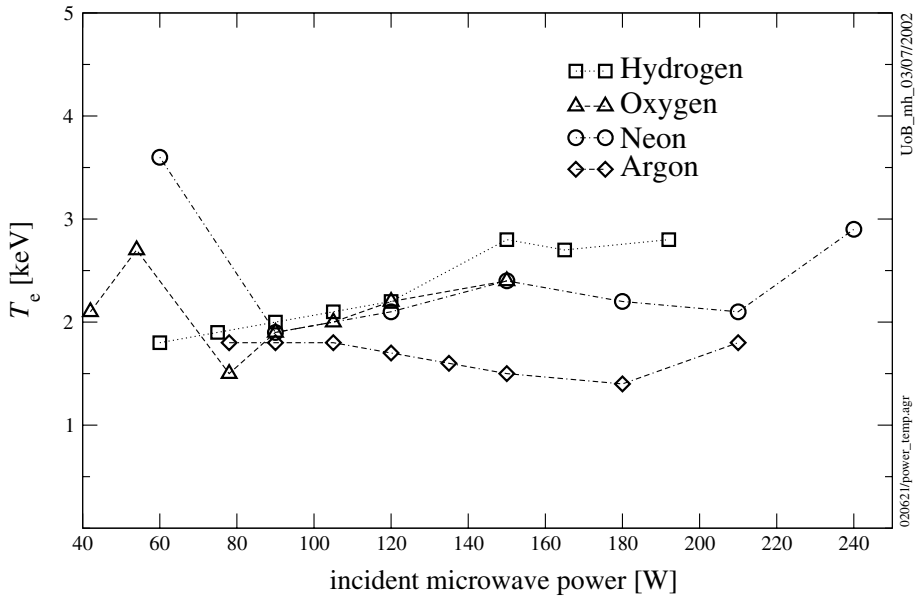

Figure 4. Temperature of the hot electron as a function of the incident microwave power measured for hydrogen H_2, oxygen O_2, neon and argon plasmas.

to the remaining data, the continuum bremsstrahlung, yielding an electron temperature of about $T_e = 1.7$ keV in this case.

In figure 4 we show the electron temperatures derived from the bremsstrahlung spectra for different operating gases (H_2, O_2, Ne and Ar) and for different incident microwave powers. The temperature of the hot electron is plotted as a function of the incident microwave power. There are two main results: first the electron temperature does not change significantly with increasing microwave power. Although one would expect a positive relationship of the temperature with microwave power, it is known that the high-energy electrons are pushed into the loss cone of the magnetic confinement by the microwave field and thus the hot electrons are lost [14]. Such a flat response with increasing microwave power, above an initial rise, has been observed in other ECR sources, though at higher electron temperatures because of the higher microwave frequencies used in these sources [8, 9]. The second result is that the electron temperature amounts to about $T_e \approx 2$ keV for all four gases. The accuracy of the T_{e1} determinations is estimated to be about 30%. If we consider the scattering of photons from the chamber wall, which is less than 25%, this will reduce the electron temperature by about 10% [6]. Note that this electron temperature is in good agreement with recent measurements of T_{e1} ranging from 3 to 5 keV from [6, 7, 15], considering that that group used a 7.25 GHz ECR ion source. In addition to this hot electron population a second population is typically found with electron temperatures T_{e2} in the range of 25–80 keV [6–9, 15]. Given the much higher temperature of the second population, the hot population with T_{e1} is often referred to as the 'warm' electron population.

3.2. Electron density

The density of the hot electrons can be estimated from the bremsstrahlung spectra by measuring absolute intensities and absolute count rates generated by photons. From these count rates we calculate the total bremsstrahlung power per unit volume. The total power per unit volume Q is given by integrating the spectral power, $j(\omega)$, emitted into 4π per unit frequency over all angular velocities (ω):

$$Q = \int_0^{+\infty} 4\pi j(\omega) \mathrm{d}\omega \qquad [\mathrm{W\,m^{-3}}]. \tag{2}$$

The spectral bremsstrahlung power emitted by a Maxwellian assembly of electrons into 4π per unit frequency is [16]

$$4\pi j(\omega) = n_e n_i Z^2 \left(\frac{e^2}{4\pi\epsilon_0}\right)^3 \frac{16\pi}{3\sqrt{3}\, m_e^2 c^3} \left(\frac{2m_e}{\pi T_e}\right)^{1/2} \times \exp\left(-\frac{\hbar\omega}{k_B T_e}\right) \cdot \bar{g}. \tag{3}$$

The factor $\bar{g}$ in equation (3) is the so-called Maxwell-averaged Gaunt factor, a dimensionless factor, which is generally a weakly varying quantity of order 1. It lies between 0.3 and 2 for $0.1 \leqslant \hbar\omega/k_B T_e \leqslant 10$ and is set to 1 here [16]. Z is the charge number of the ions, m_e is the electron mass, $k_B T_e$ is the mean kinetic energy of the electrons and $\hbar\omega$ stands for the energy of the photons.

In the following, all the physical constants are summarized in the constant K. The charge number Z is set to 1 assuming that the dominant ion is singly charged and that the contribution of all the multiple-charged ions is small or negligible (see figure 1). The integral (equation (2)) yields an expression for the densities of electrons and ions:

$$n_e n_i = \frac{\hbar}{K} \cdot \frac{Q}{\sqrt{k_B T_e}} \qquad [\mathrm{m^{-6}}]. \tag{4}$$

The power detected by the x-ray detector Q_{det} can be derived from the measured bremsstrahlung spectra through the total energy E_{tot} deposited in the Si-crystal during the measurement interval Δt. The same exponential fit as that for the electron temperature (see figure 3 panel (a)) allows an analytic integration of equation (1) over the photon energy

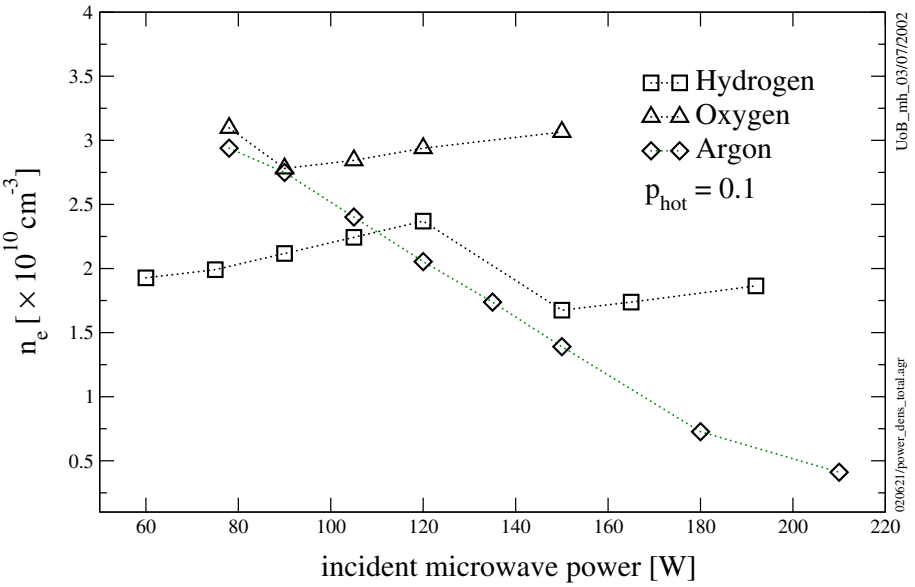

Figure 5. Estimations of the electron densities for a hydrogen, oxygen and argon plasma as a function of the incident microwave power.

($E = \hbar\omega$). The parameters A_0 and T_e obtained from these fits give the detected total photon flux from the bremsstrahlung and the temperature of the electrons.

The total power of the bremsstrahlung emitted from the plasma can be estimated by calculating the power that flows through the surface of a sphere with radius R_0 emitted from a point like plasma. The detector being located on this sphere covers 5 mm^2 (S_{det}) obtaining a power of Q_{det}. This specific power has to be divided by the volume of our plasma V_{plasma}, which is estimated to be an ellipsoid of revolution ($a = b = 1.5$ cm, $c = 3$ cm), based on the magnetic resonance surface, leading to

$$Q = \frac{3R_0^2}{a^2 c} \cdot \frac{A_0}{S_{det}\Delta t} \cdot k_B T_e \qquad [\mathrm{W\,m^{-3}}]. \tag{5}$$

Finally, we insert equation (5) into equation (4) and obtain an expression for the product of the electron and ion densities. The electron and ion densities are supposed to be equal because of the charge neutrality of the plasma. Only the hot electron population contributes to the bremsstrahlung spectrum, while the cold population contributes photons with energies which are below the detection limit of 1 keV of our detector. Thus, to get a value for the whole electron population the fraction of the hot electrons, p_{hot}, is considered yielding the following equation:

$$n_e = \sqrt{\frac{K_0 A_0}{\Delta t\, p_{hot}} \cdot \sqrt{k_B T_e}} \qquad [\mathrm{m^{-3}}]. \tag{6}$$

All physical constants are gathered in K_0 together with the fixed experiment parameters R_0, a, c and S_{det}. The fraction of hot electrons p_{hot} was found to be between 0.01 and 0.1 according to already published values [1,8,17] and our plasma model [10]. Our ECR plasma model calculates the ion charge state densities in the plasma together with the electron densities in a self-consistant way, assuming two Maxwellian electron distributions, a cold and a hot electron population. The measured charge state distribution in the extracted ion current is one of several experimental parameters to constrain the model [10].

In figure 5 measurements of the electron density (and of the density of singly charged ions) as a function of the incident microwave power for a hydrogen, oxygen and argon plasma are shown. The total electron densities obtained from x-ray measurements are in the range of (0.5–3) $\times$ 10^{10} cm^{-3} for $p_{hot} = 0.1$. The accuracy of the density determination is influenced by two parameters that are not known well: the Gaunt factor of equation (3) and the fraction of hot electrons entering in equation (6). Both $\bar{g}$ and p_{hot} influence the density calculation by their square root. For $p_{hot} = 0.01$ the densities are a factor of 3 higher. These density values are in good agreement with published values [1,8,17] and our simulations [10].

For hydrogen and oxygen the electron density remains at the same value for all incident powers with the electron density for oxygen being about 40% higher than for hydrogen. One reason for this difference may be that all the hydrogen ions are only singly charged while the oxygen ions can be multiple charged. The multiple charged oxygen ions contribute to the electron density with more than one electron per ion than the singly charged hydrogen ions. This higher contribution leads to a higher electron density. There is no significant change in the electron density when increasing the incident microwave power. The densities probably have reached the maximum possible value. More power generates stronger reflections, and thus the plasma becomes unstable, leading finally to a breakdown of the plasma discharge. For the hydrogen measurements a power breakdown occurred for an incident microwave power of 160 W, and no more data could be recorded due to intensive reflections. The same breakdown occurred for oxygen at a power of 200 W.

The behaviour of the electron density for the argon plasma is different from that for hydrogen and oxygen. While the microwave power increases from 80 to 210 W the electron density decreases by almost a factor of 10. One difference

is that Ar is an atom, whereas O_2 and H_2 are molecules. A dissociation of these molecules occurs and may influence the plasma parameters. Perhaps the higher microwave power leads to a lower ionization efficiency, e.g. due to a less quiescent plasma generated by intensive reflections of the microwave power and thus to fewer multiple charged ions and finally to a lower electron density. Compared with all other gases, argon showed for a variety of plasma parameters often a different behaviour which complicates the interpretation of measurements.

4. Summary

The detection of bremsstrahlung emitted by an ECRIS plasma with a small state-of-the-art x-ray detector revealed a high temperature for a small fraction of the total electron population. The temperature of these hot electrons is about 1.5–3 keV, which is in good agreement with recent measurements of T_{e1} ranging from 3 to 5 keV from [6, 7, 15]. With regard to other reports in the literature, this temperature seems to be very high. Electron temperatures between 10 and 35 eV were reported by [18–20] and values even lower than 10 eV for comparable 2.45 GHz ECRIS [1, 21, 22]. An important point is that the literature values are mean temperatures of the whole electron population, and no differentiation between a hot and a cold electron population is made. If we were to give such a mean temperature for the whole electron population for our ECRIS it would be below 50 eV as well, since the fraction of hot electrons is small and the temperature of the large cold electron population was simulated to be less than 2 eV [10]. The same cold temperature was found by Wiesemann from spectroscopic measurements but for a smaller fraction of the cold electrons ($p_{cold} = 0.5$–0.8) [23].

The fraction of the hot electrons in our source is estimated to be in the range $p_{hot} = 0.01$–0.1 [10]. In the literature one finds several studies in which electron temperatures and fractions of cold and hot electron populations are presented, but all of them are measured in ECR ion sources operated at frequencies higher than our 2.45 GHz. Alton and Smithe [17] use a 8 GHz ECRIS and measure $T_{cold} = 1$ eV, $T_{hot} = 100$ eV and $p_{hot} = 0.01$, Girard *et al* [8] use 10–18 GHz with $T_{hot} = 80$ keV and $p_{hot} = 0.1$, Golubev *et al* [24] use 37.5 GHz with $T_{cold} = 300$–400 eV, $T_{hot} = 7$–10 keV and $p_{hot} = 4 \times 10^{-5}$ and Petty *et al* [25] use 10.5 GHz with $T_{cold} = 100$ eV, $T_{hot} = 300$ keV and $p_{hot} = 0.5$, to name only a few. These examples show two things: first the span of electron temperatures is very broad and second the colder the temperature for the cold electron population the hotter the temperature for the energetic electrons, often together with a smaller fraction. Seen in this context, our high temperature for the hot electron population is quite evident and is inevitable for the creation of highly charged ions.

The total electron density in our source is in the range of $(1$–$5) \times 10^{10}\,\mathrm{cm}^{-3}$, which is very close to the typical critical density of $8 \times 10^{10}\,\mathrm{cm}^{-3}$. Since we consider only single charged ions for the calculation of the electron density we underestimate the electron density, and a somewhat higher electron density is realistic as well and is still compatible with the critical density.

To conclude, we showed for a small and compact 2.45 GHz ECRIS that there exists a very hot but small fraction of electrons with energies up to several tens of keV. These hot temperatures do not change significantly with microwave power. Even for different gas types the temperature is about the same, which is not true for the densities of the electrons, which may vary with microwave power depending on the structure of the gas, atomic or molecular type.

Acknowledgments

The authors wish to thank J Fischer and R Liniger and their teams for the excellent work for realizing the mechanical and the electronic design, respectively, of the system. We are grateful to Professor E Salzborn from the University of Giessen (Germany) for making available the design of their 2.45 GHz ECRIS to us. This work was supported by the Swiss National Science Foundation (SNSF).

References

[1] Geller R 1996 *Electron Cyclotron Resonance Ion Sources and ECR Plasmas* (London: Institute of Physics)
[2] Girard A 1992 Plasma diagnosis related to ion sources (invited) *Rev. Sci. Instrum.* **63** 2676–82
[3] Liehr M, Trassl R, Schlapp M and Salzborn E 1992 A low power 2.45 GHz ECR ion source for multiple charged ions *Rev. Sci. Instrum.* **63** 2541–3
[4] Marti A, Schletti R, Wurz P and Bochsler P 2001 Calibration facility for solar wind plasma instrumentation *Rev. Sci. Instrum.* **72** 1354–60
[5] Bernhardi K and Wiesemann K 1982 X-ray Bremsstrahlung measurements on an ECR-discharge in a magnetic mirror *Plasma Phys.* **24** 867–84
[6] Friedlein R and Zschornack G 1994 Angle dispersive de-convolution of Bremsstrahlung spectra from plasma *Nucl. Instrum. Methods* A **349** 554–7
[7] Friedlein R, Herpich S, Hiller H, Wirth H, Zschornack G and Tyroff H 1995 Experimental study of the hot and warm electron populations in an electron cyclotron resonance argon-oxygen-hydrogen plasma *Phys. Plasmas* **2** 2138–40
[8] Girard A, Briand P, Gaudart G, Klein J P, Bourg F, Debernardi J, Mathonnet J M, Melin G and Su Y 1994 The Quadrumafios electron cyclotron resonance ion source: presentation and analysis of the results *Rev. Sci. Instrum.* **65** 1714–17
[9] Barué C, Briand P, Girard A, Melin G and Brifford G 1992 Hot electron studies in the Minimafios ECR ion source *Rev. Sci. Instrum.* **63** 2844–46
[10] Hohl M 2002 MEFISTO II: design, setup, characterization and operation of an improved calibration facility for solar plasma instrumentation *PhD Thesis* University of Bern
[11] Wurz P, Marti A and Bochsler P 1998 New test facility for solar wind instrumentation *Helv. Phys. Acta* **71** (separanda 1) 23–4
[12] William F W, Parrington J R and Feiner F 1989 *Nuclides and Isotopes* 14th edn (San Jose, CA: General Electric Company) p 46
[13] Bernhardi K 1980 An improved deconvolution method for Bremsstrahlung spectra from hot plasmas *Comput. Phys. Commun.* **19** 17–21
[14] Girard A, Hitz D, Melin G and Serebrennikov K 2004 Electron cyclotron resonance plasmas and electron cylcontron resonance ion sources: physics and technology *Rev. Sci. Instrum.* **75** 1381–8
[15] Friedlein R, Küchler D, Zippe C, Zschornack G and Tyrroff H Ê 1996 Energy dispersive x-ray spectroscopy for ECR plasma diagnostics *Hyperfine Interact.* **99** 225–34

[16] Hutchinson I H 1987 *Principles of Plasma Diagnostics* (Cambridge: Cambridge University Press)
[17] Alton G D and Smithe D N 1994 Design studies for advanced ECR ion source *Rev. Sci. Instrum.* **65** 775–87
[18] Bhattacharjee S and Amemiya H 1999 Production of microwave plasma in narrow cross sectional tubes: effect of the shape of cross section. *Rev. Sci. Instrum.* **70** 3332–7
[19] Maeda M and Amemiya H 1994 Electron cyclotron resonance plasma in multicusp magnets with axial magnetic plugging *Rev. Sci. Instrum.* **65** 3751–5
[20] Outten C A, Barbour J C and Wampler W R 1991 Characterization of electron cyclotron resonance hydrogen plasmas *J. Vac. Sci. Technol.* A **9** 717–21
[21] Cronrath W, Bowden M D, Uchino K, Muraoka K, Muta H and Yoshida M 1997 Spatial distribution of electron temperature and density in electron cyclotron resonance discharges *J. Appl. Phys.* **81** 2105–13
[22] Liu M, Hu X, Wu Q, Yu G and Pan Y 2000 Self-consistent simulation of cyclotron resonance plasma discharge *Phys. Plasmas* **7** 3062–7
[23] Wiesemann K 1996 Characterisation of plasmas by advanced diagnostic methods *Pure Appl. Chem.* **68** 1029–34
[24] Golubev S V, Razin S V, Semenov V E, Smirnov A N, Vodopyanov A V and Zorin V G 2000 Formation of multi-charged ions and plasma stability at quasigasdynamic plasma confinement in a mirror magnetic trap *Rev. Sci. Instrum.* **71** 669–71
[25] Petty C C, Goodman D L, Smatlak D L and Smith D K 1991 Confinement of multiply charged ions in a cyclotron resonance heated mirror plasma. *Phys. Fluids* B **3** 705–14